

**Measurement of the Forward-Backward Asymmetry
in the $B \rightarrow K^{(*)}\mu^+\mu^-$ Decay
and First Observation of the $B_s^0 \rightarrow \phi\mu^+\mu^-$ Decay**

- T. Aaltonen,²² B. Álvarez González^v,¹⁰ S. Amerio,⁴² D. Amidei,³³ A. Anastassov,³⁷ A. Annovi,¹⁸ J. Antos,¹³ G. Apollinari,¹⁶ J.A. Appel,¹⁶ A. Apresyan,⁴⁷ T. Arisawa,⁵⁶ A. Artikov,¹⁴ J. Asaadi,⁵² W. Ashmanskas,¹⁶ B. Auerbach,⁵⁹ A. Aurisano,⁵² F. Azfar,⁴¹ W. Badgett,¹⁶ A. Barbaro-Galtieri,²⁷ V.E. Barnes,⁴⁷ B.A. Barnett,²⁴ P. Barria^{ee},⁴⁵ P. Bartos,¹³ M. Bauce^{cc},⁴² G. Bauer,³¹ F. Bedeschi,⁴⁵ D. Beecher,²⁹ S. Behari,²⁴ G. Bellettini^{dd},⁴⁵ J. Bellinger,⁵⁸ D. Benjamin,¹⁵ A. Beretvas,¹⁶ A. Bhatti,⁴⁹ M. Binkley*,¹⁶ D. Bisello^{cc},⁴² I. Bizjakⁱⁱ,²⁹ K.R. Bland,⁵ C. Blocker,⁷ B. Blumenfeld,²⁴ A. Bocci,¹⁵ A. Bodek,⁴⁸ D. Bortoletto,⁴⁷ J. Boudreau,⁴⁶ A. Boveia,¹² B. Brau^a,¹⁶ L. Brigliadori^{bb},⁶ A. Brisuda,¹³ C. Bromberg,³⁴ E. Brucken,²² M. Bucciantonio^{dd},⁴⁵ J. Budagov,¹⁴ H.S. Budd,⁴⁸ S. Budd,²³ K. Burkett,¹⁶ G. Busetto^{cc},⁴² P. Bussey,²⁰ A. Buzatu,³² S. Cabrera^x,¹⁵ C. Calanca,³⁰ S. Camarda,⁴ M. Campanelli,³⁴ M. Campbell,³³ F. Canelli¹²,¹⁶ A. Canepa,⁴⁴ B. Carls,²³ D. Carlsmith,⁵⁸ R. Carosi,⁴⁵ S. Carrillo^k,¹⁷ S. Carron,¹⁶ B. Casal,¹⁰ M. Casarsa,¹⁶ A. Castro^{bb},⁶ P. Catastini,¹⁶ D. Cauz,⁵³ V. Cavaliere^{ee},⁴⁵ M. Cavalli-Sforza,⁴ A. Cerri^f,²⁷ L. Cerrito^q,²⁹ Y.C. Chen,¹ M. Chertok,⁸ G. Chiarelli,⁴⁵ G. Chlachidze,¹⁶ F. Chlebana,¹⁶ K. Cho,²⁶ D. Chokheli,¹⁴ J.P. Chou,²¹ W.H. Chung,⁵⁸ Y.S. Chung,⁴⁸ C.I. Ciobanu,⁴³ M.A. Ciocci^{ee},⁴⁵ A. Clark,¹⁹ D. Clark,⁷ G. Compostella^{cc},⁴² M.E. Convery,¹⁶ J. Conway,⁸ M. Corbo,⁴³ M. Cordelli,¹⁸ C.A. Cox,⁸ D.J. Cox,⁸ F. Crescioli^{dd},⁴⁵ C. Cuenca Almenar,⁵⁹ J. Cuevas^v,¹⁰ R. Culbertson,¹⁶ D. Dagenhart,¹⁶ N. d'Ascenzo^t,⁴³ M. Datta,¹⁶ P. de Barbaro,⁴⁸ S. De Cecco,⁵⁰ G. De Lorenzo,⁴ M. Dell'Orso^{dd},⁴⁵ C. Deluca,⁴ L. Demortier,⁴⁹ J. Deng^c,¹⁵ M. Deninno,⁶ F. Devoto,²² M. d'Errico^{cc},⁴² A. Di Canto^{dd},⁴⁵ B. Di Ruzza,⁴⁵ J.R. Dittmann,⁵ M. D'Onofrio,²⁸ S. Donati^{dd},⁴⁵ P. Dong,¹⁶ T. Dorigo,⁴² K. Ebina,⁵⁶ A. Elagin,⁵² A. Eppig,³³ R. Erbacher,⁸ D. Errede,²³ S. Errede,²³ N. Ershaidat^{aa},⁴³ R. Eusebi,⁵² H.C. Fang,²⁷ S. Farrington,⁴¹ M. Feindt,²⁵ J.P. Fernandez,³⁰ C. Ferrazza^{ff},⁴⁵ R. Field,¹⁷ G. Flanagan^r,⁴⁷ R. Forrest,⁸ M.J. Frank,⁵ M. Franklin,²¹ J.C. Freeman,¹⁶ I. Furic,¹⁷ M. Gallinaro,⁴⁹ J. Galyardt,¹¹ J.E. Garcia,¹⁹ A.F. Garfinkel,⁴⁷ P. Garosi^{ee},⁴⁵ H. Gerberich,²³ E. Gerchtein,¹⁶ S. Giagu^{gg},⁵⁰ V. Giakoumopoulou,³ P. Giannetti,⁴⁵ K. Gibson,⁴⁶ C.M. Ginsburg,¹⁶ N. Giokaris,³ P. Giromini,¹⁸ M. Giunta,⁴⁵ G. Giurgiu,²⁴ V. Glagolev,¹⁴ D. Glenzinski,¹⁶ M. Gold,³⁶ D. Goldin,⁵² N. Goldschmidt,¹⁷ A. Golossanov,¹⁶ G. Gomez,¹⁰ G. Gomez-Ceballos,³¹ M. Goncharov,³¹ O. González,³⁰ I. Gorelov,³⁶ A.T. Goshaw,¹⁵ K. Goulianos,⁴⁹ A. Gresele,⁴² S. Grinstein,⁴ C. Grossi-Pilcher,¹² R.C. Group,¹⁶ J. Guimaraes da Costa,²¹ Z. Gunay-Unalan,³⁴ C. Haber,²⁷ S.R. Hahn,¹⁶ E. Halkiadakis,⁵¹ A. Hamaguchi,⁴⁰ J.Y. Han,⁴⁸ F. Happacher,¹⁸ K. Hara,⁵⁴ D. Hare,⁵¹ M. Hare,⁵⁵ R.F. Harr,⁵⁷ K. Hatakeyama,⁵ C. Hays,⁴¹ M. Heck,²⁵ J. Heinrich,⁴⁴ M. Herndon,⁵⁸ S. Hewamanage,⁵ D. Hidas,⁵¹ A. Hocker,¹⁶ W. Hopkins^g,¹⁶ D. Horn,²⁵ S. Hou,¹ R.E. Hughes,³⁸ M. Hurwitz,¹² U. Husemann,⁵⁹ N. Hussain,³² M. Hussein,³⁴ J. Huston,³⁴ G. Introzzi,⁴⁵ M. Iori^{gg},⁵⁰ A. Ivanov^o,⁸ E. James,¹⁶ D. Jang,¹¹ B. Jayatilaka,¹⁵ E.J. Jeon,²⁶ M.K. Jha,⁶ S. Jindariani,¹⁶ W. Johnson,⁸ M. Jones,⁴⁷ K.K. Joo,²⁶ S.Y. Jun,¹¹ T.R. Junk,¹⁶ T. Kamon,⁵² P.E. Karchin,⁵⁷ Y. Katoⁿ,⁴⁰ W. Ketchum,¹² J. Keung,⁴⁴ V. Khotilovich,⁵² B. Kilminster,¹⁶ D.H. Kim,²⁶ H.S. Kim,²⁶ H.W. Kim,²⁶ J.E. Kim,²⁶ M.J. Kim,¹⁸ S.B. Kim,²⁶ S.H. Kim,⁵⁴ Y.K. Kim,¹² N. Kimura,⁵⁶ S. Klimentko,¹⁷ K. Kondo,⁵⁶ D.J. Kong,²⁶ J. Konigsberg,¹⁷ A. Korytov,¹⁷ A.V. Kotwal,¹⁵ M. Kreps,²⁵ J. Kroll,⁴⁴ D. Krop,¹² N. Krumnack^l,⁵ M. Kruse,¹⁵ V. Krutelyov^d,⁵² T. Kuhr,²⁵ M. Kurata,⁵⁴ S. Kwang,¹² A.T. Laasanen,⁴⁷ S. Lami,⁴⁵ S. Lammel,¹⁶ M. Lancaster,²⁹ R.L. Lander,⁸ K. Lannon^u,³⁸ A. Lath,⁵¹ G. Latino^{ee},⁴⁵ I. Lazzizzera,⁴² T. LeCompte,² E. Lee,⁵² H.S. Lee,¹² J.S. Lee,²⁶ S.W. Lee^w,⁵² S. Leo^{dd},⁴⁵ S. Leone,⁴⁵ J.D. Lewis,¹⁶ C.-J. Lin,²⁷ J. Linacre,⁴¹ M. Lindgren,¹⁶ E. Lipeles,⁴⁴ A. Lister,¹⁹ D.O. Litvintsev,¹⁶ C. Liu,⁴⁶ Q. Liu,⁴⁷ T. Liu,¹⁶ S. Lockwitz,⁵⁹ N.S. Lockyer,⁴⁴ A. Loginov,⁵⁹ D. Lucchesi^{cc},⁴² J. Lueck,²⁵ P. Lujan,²⁷ P. Lukens,¹⁶ G. Lungu,⁴⁹ J. Lys,²⁷ R. Lysak,¹³ R. Madrak,¹⁶ K. Maeshima,¹⁶ K. Makhoul,³¹ P. Maksimovic,²⁴ S. Malik,⁴⁹ G. Manca^b,²⁸ A. Manousakis-Katsikakis,³ F. Margaroli,⁴⁷ C. Marino,²⁵ M. Martínez,⁴ R. Martínez-Ballarín,³⁰ P. Mastrandrea,⁵⁰ M. Mathis,²⁴ M.E. Mattson,⁵⁷ P. Mazzanti,⁶ K.S. McFarland,⁴⁸ P. McIntyre,⁵² R. McNultyⁱ,²⁸ A. Mehta,²⁸ P. Mehtala,²² A. Menzione,⁴⁵ C. Mesropian,⁴⁹ T. Miao,¹⁶ D. Mietlicki,³³ A. Mitra,¹ H. Miyake,⁵⁴ S. Moed,²¹ N. Moggi,⁶ M.N. Mondragon^k,¹⁶ C.S. Moon,²⁶ R. Moore,¹⁶ M.J. Morello,¹⁶ J. Morlock,²⁵ P. Movilla Fernandez,¹⁶ A. Mukherjee,¹⁶ Th. Muller,²⁵ P. Murat,¹⁶ M. Mussini^{bb},⁶ J. Nachtman^m,¹⁶ Y. Nagai,⁵⁴ J. Naganoma,⁵⁶ I. Nakano,³⁹ A. Napier,⁵⁵ J. Nett,⁵⁸ C. Neu^z,⁴⁴ M.S. Neubauer,²³ J. Nielsen^e,²⁷ L. Nodulman,² O. Norniella,²³ E. Nurse,²⁹ L. Oakes,⁴¹ S.H. Oh,¹⁵ Y.D. Oh,²⁶ I. Oksuzian,¹⁷ T. Okusawa,⁴⁰ R. Orava,²² L. Ortolan,⁴ S. Pagan Griso^{cc},⁴² C. Pagliarone,⁵³ E. Palencia^f,¹⁰ V. Papadimitriou,¹⁶ A.A. Paramonov,² J. Patrick,¹⁶ G. Paulette^{hh},⁵³ M. Paulini,¹¹ C. Paus,³¹ D.E. Pellett,⁸

A. Penzo,⁵³ T.J. Phillips,¹⁵ G. Piacentino,⁴⁵ E. Pianori,⁴⁴ J. Pilot,³⁸ K. Pitts,²³ C. Plager,⁹ L. Pondrom,⁵⁸ K. Potamianos,⁴⁷ O. Poukhov*,¹⁴ F. Prokoshin^y,¹⁴ A. Pronko,¹⁶ F. Ptahos^h,¹⁸ E. Pueschel,¹¹ G. Punzi^{dd},⁴⁵ J. Pursley,⁵⁸ A. Rahaman,⁴⁶ V. Ramakrishnan,⁵⁸ N. Ranjan,⁴⁷ I. Redondo,³⁰ P. Renton,⁴¹ M. Rescigno,⁵⁰ F. Rimondi^{bb},⁶ L. Ristori⁴⁵,¹⁶ A. Robson,²⁰ T. Rodrigo,¹⁰ T. Rodriguez,⁴⁴ E. Rogers,²³ S. Rolli,⁵⁵ R. Roser,¹⁶ M. Rossi,⁵³ F. Ruffini^{ee},⁴⁵ A. Ruiz,¹⁰ J. Russ,¹¹ V. Rusu,¹⁶ A. Safonov,⁵² W.K. Sakamoto,⁴⁸ L. Santi^{hh},⁵³ L. Sartori,⁴⁵ K. Sato,⁵⁴ V. Saveliev^t,⁴³ A. Savoy-Navarro,⁴³ P. Schlabach,¹⁶ A. Schmidt,²⁵ E.E. Schmidt,¹⁶ M.P. Schmidt*,⁵⁹ M. Schmitt,³⁷ T. Schwarz,⁸ L. Scodellaro,¹⁰ A. Scribano^{ee},⁴⁵ F. Scuri,⁴⁵ A. Sedov,⁴⁷ S. Seidel,³⁶ Y. Seiya,⁴⁰ A. Semenov,¹⁴ F. Sforza^{dd},⁴⁵ A. Sfyrla,²³ S.Z. Shalhout,⁸ T. Shears,²⁸ P.F. Shepard,⁴⁶ M. Shimojima^s,⁵⁴ S. Shiraishi,¹² M. Shochet,¹² I. Shreyber,³⁵ A. Simonenko,¹⁴ P. Sinervo,³² A. Sissakian*,¹⁴ K. Sliwa,⁵⁵ J.R. Smith,⁸ F.D. Snider,¹⁶ A. Soha,¹⁶ S. Somalwar,⁵¹ V. Sorin,⁴ P. Squillacioti,¹⁶ M. Stanitzki,⁵⁹ R. St. Denis,²⁰ B. Stelzer,³² O. Stelzer-Chilton,³² D. Stentz,³⁷ J. Strologas,³⁶ G.L. Strycker,³³ Y. Sudo,⁵⁴ A. Sukhanov,¹⁷ I. Suslov,¹⁴ K. Takemasa,⁵⁴ Y. Takeuchi,⁵⁴ J. Tang,¹² M. Tecchio,³³ P.K. Teng,¹ J. Thom^g,¹⁶ J. Thome,¹¹ G.A. Thompson,²³ E. Thomson,⁴⁴ P. Tito-Guzmán,³⁰ S. Tkaczyk,¹⁶ D. Toback,⁵² S. Tokar,¹³ K. Tollefson,³⁴ T. Tomura,⁵⁴ D. Tonelli,¹⁶ S. Torre,¹⁸ D. Torretta,¹⁶ P. Totaro^{hh},⁵³ M. Trovato^{ff},⁴⁵ Y. Tu,⁴⁴ N. Turini^{ee},⁴⁵ F. Ukegawa,⁵⁴ S. Uozumi,²⁶ A. Varganov,³³ E. Vataga^{ff},⁴⁵ F. Vázquez^k,¹⁷ G. Velev,¹⁶ C. Vellidis,³ M. Vidal,³⁰ I. Vila,¹⁰ R. Vilar,¹⁰ M. Vogel,³⁶ G. Volpi^{dd},⁴⁵ P. Wagner,⁴⁴ R.L. Wagner,¹⁶ T. Wakisaka,⁴⁰ R. Wallny,⁹ S.M. Wang,¹ A. Warburton,³² D. Waters,²⁹ M. Weinberger,⁵² W.C. Wester III,¹⁶ B. Whitehouse,⁵⁵ D. Whiteson^c,⁴⁴ A.B. Wicklund,² E. Wicklund,¹⁶ S. Wilbur,¹² F. Wick,²⁵ H.H. Williams,⁴⁴ J.S. Wilson,³⁸ P. Wilson,¹⁶ B.L. Winer,³⁸ P. Wittich^g,¹⁶ S. Wolbers,¹⁶ H. Wolfe,³⁸ T. Wright,³³ X. Wu,¹⁹ Z. Wu,⁵ K. Yamamoto,⁴⁰ J. Yamaoka,¹⁵ T. Yang,¹⁶ U.K. Yang^p,¹² Y.C. Yang,²⁶ W.-M. Yao,²⁷ G.P. Yeh,¹⁶ K. Yi^m,¹⁶ J. Yoh,¹⁶ K. Yorita,⁵⁶ T. Yoshida^j,⁴⁰ G.B. Yu,¹⁵ I. Yu,²⁶ S.S. Yu,¹⁶ J.C. Yun,¹⁶ A. Zanetti,⁵³ Y. Zeng,¹⁵ and S. Zucchelli^{bb}

(CDF Collaboration[†])

¹*Institute of Physics, Academia Sinica, Taipei, Taiwan 11529, Republic of China*

²*Argonne National Laboratory, Argonne, Illinois 60439, USA*

³*University of Athens, 157 71 Athens, Greece*

⁴*Institut de Fisica d'Altes Energies, Universitat Autònoma de Barcelona, E-08193, Bellaterra (Barcelona), Spain*

⁵*Baylor University, Waco, Texas 76798, USA*

⁶*Istituto Nazionale di Fisica Nucleare Bologna, ^{bb}University of Bologna, I-40127 Bologna, Italy*

⁷*Brandeis University, Waltham, Massachusetts 02254, USA*

⁸*University of California, Davis, Davis, California 95616, USA*

⁹*University of California, Los Angeles, Los Angeles, California 90024, USA*

¹⁰*Instituto de Fisica de Cantabria, CSIC-University of Cantabria, 39005 Santander, Spain*

¹¹*Carnegie Mellon University, Pittsburgh, Pennsylvania 15213, USA*

¹²*Enrico Fermi Institute, University of Chicago, Chicago, Illinois 60637, USA*

¹³*Comenius University, 842 48 Bratislava, Slovakia; Institute of Experimental Physics, 040 01 Kosice, Slovakia*

¹⁴*Joint Institute for Nuclear Research, RU-141980 Dubna, Russia*

¹⁵*Duke University, Durham, North Carolina 27708, USA*

¹⁶*Fermi National Accelerator Laboratory, Batavia, Illinois 60510, USA*

¹⁷*University of Florida, Gainesville, Florida 32611, USA*

¹⁸*Laboratori Nazionali di Frascati, Istituto Nazionale di Fisica Nucleare, I-00044 Frascati, Italy*

¹⁹*University of Geneva, CH-1211 Geneva 4, Switzerland*

²⁰*Glasgow University, Glasgow G12 8QQ, United Kingdom*

²¹*Harvard University, Cambridge, Massachusetts 02138, USA*

²²*Division of High Energy Physics, Department of Physics,*

University of Helsinki and Helsinki Institute of Physics, FIN-00014, Helsinki, Finland

²³*University of Illinois, Urbana, Illinois 61801, USA*

²⁴*The Johns Hopkins University, Baltimore, Maryland 21218, USA*

²⁵*Institut für Experimentelle Kernphysik, Karlsruhe Institute of Technology, D-76131 Karlsruhe, Germany*

²⁶*Center for High Energy Physics: Kyungpook National University,*

Daegu 702-701, Korea; Seoul National University, Seoul 151-742,

Korea; Sungkyunkwan University, Suwon 440-746,

Korea; Korea Institute of Science and Technology Information,

Daejeon 305-806, Korea; Chonnam National University, Gwangju 500-757,

Korea; Chonbuk National University, Jeonju 561-756, Korea

²⁷*Ernest Orlando Lawrence Berkeley National Laboratory, Berkeley, California 94720, USA*

²⁸*University of Liverpool, Liverpool L69 7ZE, United Kingdom*

²⁹*University College London, London WC1E 6BT, United Kingdom*

³⁰*Centro de Investigaciones Energeticas Medioambientales y Tecnologicas, E-28040 Madrid, Spain*

- ³¹*Massachusetts Institute of Technology, Cambridge, Massachusetts 02139, USA*
- ³²*Institute of Particle Physics: McGill University, Montréal, Québec, Canada H3A 2T8; Simon Fraser University, Burnaby, British Columbia, Canada V5A 1S6; University of Toronto, Toronto, Ontario, Canada M5S 1A7; and TRIUMF, Vancouver, British Columbia, Canada V6T 2A3*
- ³³*University of Michigan, Ann Arbor, Michigan 48109, USA*
- ³⁴*Michigan State University, East Lansing, Michigan 48824, USA*
- ³⁵*Institution for Theoretical and Experimental Physics, ITEP, Moscow 117259, Russia*
- ³⁶*University of New Mexico, Albuquerque, New Mexico 87131, USA*
- ³⁷*Northwestern University, Evanston, Illinois 60208, USA*
- ³⁸*The Ohio State University, Columbus, Ohio 43210, USA*
- ³⁹*Okayama University, Okayama 700-8530, Japan*
- ⁴⁰*Osaka City University, Osaka 588, Japan*
- ⁴¹*University of Oxford, Oxford OX1 3RH, United Kingdom*
- ⁴²*Istituto Nazionale di Fisica Nucleare, Sezione di Padova-Trento, I-35131 Padova, Italy*
- ⁴³*LPNHE, Université Pierre et Marie Curie/IN2P3-CNRS, UMR7585, Paris, F-75252 France*
- ⁴⁴*University of Pennsylvania, Philadelphia, Pennsylvania 19104, USA*
- ⁴⁵*Istituto Nazionale di Fisica Nucleare Pisa, dd University of Pisa, ee University of Siena and ff Scuola Normale Superiore, I-56127 Pisa, Italy*
- ⁴⁶*University of Pittsburgh, Pittsburgh, Pennsylvania 15260, USA*
- ⁴⁷*Purdue University, West Lafayette, Indiana 47907, USA*
- ⁴⁸*University of Rochester, Rochester, New York 14627, USA*
- ⁴⁹*The Rockefeller University, New York, New York 10065, USA*
- ⁵⁰*Istituto Nazionale di Fisica Nucleare, Sezione di Roma 1, gg Sapienza Università di Roma, I-00185 Roma, Italy*
- ⁵¹*Rutgers University, Piscataway, New Jersey 08855, USA*
- ⁵²*Texas A&M University, College Station, Texas 77843, USA*
- ⁵³*Istituto Nazionale di Fisica Nucleare Trieste/Udine, I-34100 Trieste, hh University of Trieste/Udine, I-33100 Udine, Italy*
- ⁵⁴*University of Tsukuba, Tsukuba, Ibaraki 305, Japan*
- ⁵⁵*Tufts University, Medford, Massachusetts 02155, USA*
- ⁵⁶*Waseda University, Tokyo 169, Japan*
- ⁵⁷*Wayne State University, Detroit, Michigan 48201, USA*
- ⁵⁸*University of Wisconsin, Madison, Wisconsin 53706, USA*
- ⁵⁹*Yale University, New Haven, Connecticut 06520, USA*

We reconstruct the rare decays $B^+ \rightarrow K^+ \mu^+ \mu^-$, $B^0 \rightarrow K^*(892)^0 \mu^+ \mu^-$, and $B_s^0 \rightarrow \phi(1020) \mu^+ \mu^-$ in a data sample corresponding to 4.4 fb^{-1} collected in $p\bar{p}$ collisions at $\sqrt{s} = 1.96 \text{ TeV}$ by the CDF II detector at the Tevatron Collider. Using 121 ± 16 $B^+ \rightarrow K^+ \mu^+ \mu^-$ and 101 ± 12 $B^0 \rightarrow K^{*0} \mu^+ \mu^-$ decays we report the branching ratios. In addition, we report the differential branching ratio and the muon forward-backward asymmetry in the B^+ and B^0 decay modes, and the K^{*0} longitudinal polarization fraction in the B^0 decay mode with respect to the squared dimuon mass. These are consistent with the predictions, and most recent determinations from other experiments and of comparable accuracy. We also report the first observation of the $B_s^0 \rightarrow \phi \mu^+ \mu^-$ decay and measure its branching ratio $\text{BR}(B_s^0 \rightarrow \phi \mu^+ \mu^-) = [1.44 \pm 0.33 \pm 0.46] \times 10^{-6}$ using 27 ± 6 signal events. This is currently the most rare B_s^0 decay observed.

PACS numbers: 13.25 Hw, 13.20 He

*Deceased

[†]With visitors from ^aUniversity of Massachusetts Amherst, Amherst, Massachusetts 01003, ^bIstituto Nazionale di Fisica Nucleare, Sezione di Cagliari, 09042 Monserrato (Cagliari), Italy, ^cUniversity of California Irvine, Irvine, CA 92697, ^dUniversity of California Santa Barbara, Santa Barbara, CA 93106, ^eUniversity of California Santa Cruz, Santa Cruz, CA 95064, ^fCERN, CH-1211 Geneva, Switzerland, ^gCornell University, Ithaca, NY 14853, ^hUniversity of Cyprus, Nicosia CY-1678, Cyprus, ⁱUniversity College Dublin, Dublin 4, Ireland, ^jUniversity of Fukui, Fukui City, Fukui Prefecture, Japan 910-0017, ^kUniversidad Iberoamericana, Mexico D.F., Mexico, ^lIowa State University, Ames, IA 50011,

^mUniversity of Iowa, Iowa City, IA 52242, ⁿKinki University, Higashi-Osaka City, Japan 577-8502, ^oKansas State University, Manhattan, KS 66506, ^pUniversity of Manchester, Manchester M13 9PL, England, ^qQueen Mary, University of London, London, E1 4NS, England, ^rMuons, Inc., Batavia, IL 60510, ^sNagasaki Institute of Applied Science, Nagasaki, Japan, ^tNational Research Nuclear University, Moscow, Russia, ^uUniversity of Notre Dame, Notre Dame, IN 46556, ^vUniversidad de Oviedo, E-33007 Oviedo, Spain, ^wTexas Tech University, Lubbock, TX 79609, ^xIFIC(CSIC-Universitat de Valencia), 56071 Valencia, Spain, ^yUniversidad Técnica Federico Santa María, 110v Valparaíso, Chile, ^zUniversity of

The flavor-changing neutral current process $b \rightarrow s\ell\ell$ occurs in the standard model (SM) through higher order diagrams where new physics contributions could arise. Accurate SM predictions make the $b \rightarrow s\ell\ell$ phenomenology suited to uncover early indications of new physics [1–3], especially through observables like the lepton forward-backward asymmetry (A_{FB}) and the differential branching fraction (BR) as a function of dilepton mass $M_{\ell\ell}$. The $b \rightarrow s\ell\ell$ amplitudes can be described in terms of short distance operators and effective Wilson coefficients $C_{7,9,10}$. Some new physics models [1] allow the flipped sign of C_7 . This results in the opposite sign of A_{FB} in the small q^2 region ($q^2 \equiv M_{\ell\ell}^2 c^2$). Recently, BaBar and Belle [4] measured an A_{FB} in the $B^0 \rightarrow K^{*0}\ell^+\ell^-$ decay larger than the SM expectation. The decay $B_s^0 \rightarrow \phi(1020)\mu^+\mu^-$ has not been seen in previous searches by CDF [5] and D0 [6].

In this Letter we report an update of our previous analysis [5] of the rare decay modes $B^+ \rightarrow K^+\mu^+\mu^-$, $B^0 \rightarrow K^{*0}\mu^+\mu^-$, and $B_s^0 \rightarrow \phi\mu^+\mu^-$ using an increased data sample of $p\bar{p}$ collisions at a center-of-mass energy of $\sqrt{s} = 1.96$ TeV corresponding to an integrated luminosity of 4.4 fb^{-1} , collected with the CDF II detector between March 2002 and January 2009. We update the BR measurements and also report the measurement of A_{FB} in the $B^0 \rightarrow K^{*0}\mu^+\mu^-$ decay.

We reconstruct $B \rightarrow h\mu^+\mu^-$ candidates, where B stands for B^+ , B^0 , or B_s^0 , and h stands for K^+ , K^{*0} , or ϕ , respectively. Charge-conjugation is implied throughout the Letter. The K^{*0} (ϕ) meson is reconstructed in the decay $K^{*0} \rightarrow K^+\pi^-$ ($\phi \rightarrow K^+K^-$). We also reconstruct $B \rightarrow J/\psi h$ decays as normalization channels in BR measurements, because they have final states identical to those of the signals, resulting in a cancellation of many systematic uncertainties. The relative BR's are:

$$\frac{\text{BR}(B \rightarrow h\mu^+\mu^-)}{\text{BR}(B \rightarrow J/\psi h)} = \frac{N_{h\mu^+\mu^-}}{N_{J/\psi h}} \frac{\varepsilon_{J/\psi h}}{\varepsilon_{h\mu^+\mu^-}} \times \text{BR}(J/\psi \rightarrow \mu^+\mu^-), \quad (1)$$

where $N_{h\mu^+\mu^-}$ ($N_{J/\psi h}$) is the $B \rightarrow h\mu^+\mu^-$ ($B \rightarrow J/\psi h$) yield, and $\varepsilon_{h\mu^+\mu^-}/\varepsilon_{J/\psi h}$ is the relative reconstruction efficiency determined from the simulation.

The CDF II detector is described in detail in Ref. [7] with the detector subsystems relevant for this analysis discussed in Ref. [8].

A sample of dimuon events is selected by the online trigger system. The trigger requires two opposite charged particles with transverse momentum $p_T \geq 1.5$ or $2.0 \text{ GeV}/c$ depending on the trigger condition, matched to the muon chambers. We use the muon chambers detect muons within $|\eta| < 0.6$ and $0.6 < |\eta| < 1.0$ [9].

The trigger also requires $L_{xy} > 200 \mu\text{m}$, where L_{xy} is the transverse displacement of their intersection from the beamline. The detail of the trigger system and selection requirements can be found in Ref. [5].

The offline loose event selection begins by looking for a common vertex of two trigger muons with one (two opposite-charge) reconstructed charged particle(s) to form a $B^+ \rightarrow K^+\mu^+\mu^-$ (a $B^0 \rightarrow K^{*0}\mu^+\mu^-$ or a $B_s^0 \rightarrow \phi\mu^+\mu^-$) candidate. The probability of the vertex fit χ^2 is required to be greater than 10^{-3} . All charged particle trajectories are required to be associated with hits in the silicon vertex detector and to have $p_T \geq 0.4 \text{ GeV}/c$. In addition, we require $p_T(h) \geq 1.0 \text{ GeV}/c$ and $p_T(B) \geq 4.0 \text{ GeV}/c$. We require that the B candidate's decay is consistent with being displaced from the primary interaction point in the transverse plane by $L_{xy}(B)/\sigma(L_{xy}(B)) \geq 3$, and $\sigma(L_{xy}(B))$ is the estimated uncertainty of $L_{xy}(B)$. We also require that the B candidate comes from the primary vertex by $|d_0(B)| \leq 120 \mu\text{m}$, where $d_0(B)$ is the distance of closest approach of the B trajectory to the beamline.

For B^0 (B_s^0) candidates the $K^+\pi^-$ (K^+K^-) mass must lie within 50 (10) MeV/c^2 of the world average K^{*0} (ϕ) mass [10]. The ambiguity of the mass assignment in the $K^{*0} \rightarrow K^+\pi^-$ decay is handled by choosing the combination with the $K^+\pi^-$ mass closer to the known K^{*0} mass. This results in the correct mass assignments for about 92% of the decays as determined from the simulation. Particle identification is performed with the time-of-flight and the ionization energy loss (dE/dx) probabilities of the particle hypothesis. We require loose particle identification for both kaons and pions coming from the K^{*0} meson or ϕ meson to reduce combinatorial background. This removes 15% of the B mass sideband events while 99.5% of the signal is retained. We also require a muon likelihood [11] to suppress hadron tracks that produce false trigger muons.

Rare decay candidates with a dimuon mass near the J/ψ (ψ') are rejected: 8.68 (12.86) $< q^2 < 10.09$ (14.18) GeV^2/c^2 . To eliminate the radiative charmonium decays that escaped rejection above, we remove candidates consistent with originating from a $B \rightarrow J/\psi(')h$ decay followed by the decay of the $J/\psi(')$ into two muons and a photon: $|M(\mu\mu h) - M_B^{\text{PDG}} - (M(\mu\mu) - M_{J/\psi(')}^{\text{PDG}})| < 100 \text{ MeV}/c^2$, where the PDG superscript indicates known experimental averages [10] and $M(\mu\mu) < M_{J/\psi(')}^{\text{PDG}}$. We also reject candidates if an opposite sign hadron-muon combination of the daughters, assigned the muon mass, satisfy J/ψ or ψ' mass within $40 \text{ MeV}/c^2$. This removes charmonium decays where one of the muons is misidentified as a hadron. We reject candidates in which two (three) track combinations are compatible within $\pm 25 \text{ MeV}/c^2$ with $D^0 \rightarrow K^-\pi^+$ ($D^+ \rightarrow K^-\pi^+\pi^+$ or $D_s^+ \rightarrow K^+K^-\pi^+$) decays for B^+ , B^0 , and B_s^0 decays, respectively. This removes $B \rightarrow D\pi$ ($D = D^0$, D^+ , and D_s^+) decays where

Virginia, Charlottesville, VA 22906, ^{aa}Yarmouk University, Irbid 211-63, Jordan, ⁱⁱOn leave from J. Stefan Institute, Ljubljana, Slovenia,

two hadrons are misidentified as muons.

We train an Artificial Neural Network (NN) classifier on simulated signal and a sample of events representative of the background events in the signal region. To simulate the signal we use PYTHIA and EVTGEN [12] based on the SM expectation [1]. The background sample is obtained from the sidebands of the B invariant mass distribution. We take only the higher mass sideband for the B^+ and B^0 decays since the lower sideband is populated with physics background from partially reconstructed B meson decays. We use both sidebands for B_s^0 decays. We use 7–10 observables based on B and daughter’s kinematics (e.g. p_T and mass), vertex qualities, and muon likelihoods. We optimize the NN threshold in order to maximize both the BR and the A_{FB} significance. For the B^+ and B^0 analysis we optimize the NN threshold by maximizing $N_s/\sqrt{N_s + N_b}$, where N_s (N_b) is the expected number of signal (background) events. We determine N_s by Eq. (1) with the world average BR and NN cut efficiency of the simulated signal events, and determine N_b from the number of sideband events scaled to the signal region, which is defined as $\pm 2\sigma$ from the world average B mass, and NN cut efficiency of the sideband events. For B_s^0 decays, N_s is taken from a theoretical prediction [13]. We maximize $N_s/(5/2 + \sqrt{N_b})$ [14].

The signal yield is obtained by an unbinned maximum log-likelihood fit to the B candidate invariant mass distribution. The likelihood is given by $\mathcal{L} = \prod(f_{\text{sig}}\mathcal{P}_{\text{sig}} + (1 - f_{\text{sig}})\mathcal{P}_{\text{bg}})$, where f_{sig} is the signal fraction, \mathcal{P}_{sig} is the signal probability density functions (PDF) parametrized with two Gaussian distributions with different means, and \mathcal{P}_{bg} is the background PDF modeled with a first- or second-order polynomial. The signal PDF’s are determined from the simulated signal and the B mass resolution is scaled by the ratio of the mass resolution in $J/\psi h$ data and simulation, which ranges from 1.07 to 1.09. The background PDF’s are determined from sideband data. Fitted parameters are f_{sig} , the mean B mass, and the background shape. The fit range for B^+ and B^0 (B_s^0) decays is from 5.18 (5.00) to 5.70 GeV/c², to avoid the region dominated by the physics background.

While the contribution from charmless B decays is negligible due to the muon identification, we find a sizeable crosstalk between $B^0 \rightarrow K^{*0}\mu^+\mu^-$ and $B_s^0 \rightarrow \phi\mu^+\mu^-$ contributing approximately 1% of the signal, as estimated from simulation. These contributions, whose fractions are determined by simulation assuming the world average BR and the theoretical prediction [13], are subtracted from the fit results for the signal yields.

By optimized NN threshold we reject 99.5–99.8% of background events in the signal region. Figure 1 shows the B mass distributions. The statistical significance is $s \equiv \sqrt{-2 \ln(\mathcal{L}_{\text{null}}/\mathcal{L}_{\text{max}})}$, where \mathcal{L}_{max} is obtained from a fit with the signal fraction free to float and the mean B meson mass fixed to the fitted value in the corresponding

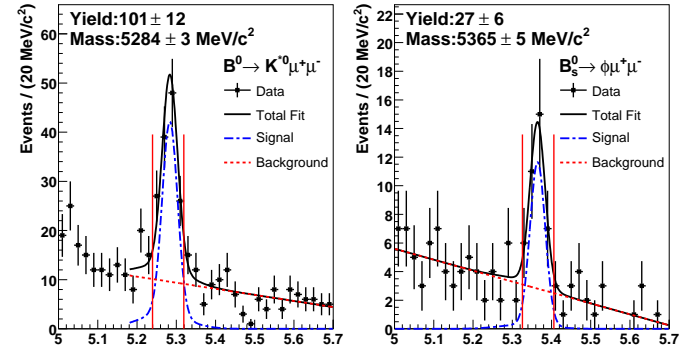


FIG. 1: Mass of $B^0 \rightarrow K^{*0}\mu^+\mu^-$ and $B_s^0 \rightarrow \phi\mu^+\mu^-$ candidates with fit results overlaid. The vertical lines show the signal region.

normalization channel, and $\mathcal{L}_{\text{null}}$ is the maximum likelihood obtained from a fit with $f_{\text{sig}} = 0$. Systematic uncertainty is not considered in the significance evaluation. We obtain $s = 8.5\sigma$, 9.7σ , and 6.3σ for B^+ , B^0 , and B_s^0 decays, respectively. The observed yields are listed in Table I. This is the first observation of the $B_s^0 \rightarrow \phi\mu^+\mu^-$ mode.

TABLE I: Summary of observed yields. The numbers in parentheses are the number of events in the signal region.

Mode	$N_{h\mu^+\mu^-}$	$N_{J/\psi h}$	$\varepsilon_{h\mu^+\mu^-}/\varepsilon_{J/\psi h}$
B^+	121 ± 16 (218)	43704 ± 245 (55296)	0.434 ± 0.006
B^0	101 ± 12 (140)	15815 ± 178 (22952)	0.477 ± 0.009
B_s^0	27 ± 6 (40)	2930 ± 64 (3883)	0.498 ± 0.012

We do not apply a NN selection to $J/\psi h$ channels, because these signals are of sufficient size and purity with the loose selection. To obtain the relative efficiency of Eq. (1), the NN cut efficiency of the loosely selected events is considered in addition to the relative efficiency of the loose selection.

The dominant source of systematic uncertainty for each BR measurement is the background PDF parameterization (3.9%) for B^+ , the discrepancy of the NN cut efficiency between data and simulation (4.8%) for B^0 , and particle identification (3.5%) for B_s^0 . For the absolute BR measurements we assign the uncertainties of the world average BR($B \rightarrow J/\psi h$) [10].

Results of the relative BR (Eq. (1)) measurements are listed in Table II. The BR statistical uncertainties include the Poisson term from finite statistics of the sample. We also show the absolute BR which is obtained by replacing the normalization channel’s BR with the corresponding world average [10] value.

These numbers are consistent with our previous results [5], B-factory measurements [4, 15], and theoretical expectations [13]. We also measure differential BRs with

TABLE II: Measured branching fractions of rare modes. First (second) uncertainty is statistical (systematic).

Mode	Relative BR(10^{-3})	Absolute BR(10^{-6})
$B^+ \rightarrow K^+ \mu^+ \mu^-$	$0.38 \pm 0.05 \pm 0.02$	$0.38 \pm 0.05 \pm 0.03$
$B^0 \rightarrow K^{*0} \mu^+ \mu^-$	$0.80 \pm 0.10 \pm 0.06$	$1.06 \pm 0.14 \pm 0.09$
$B_s^0 \rightarrow \phi \mu^+ \mu^-$	$1.11 \pm 0.25 \pm 0.09$	$1.44 \pm 0.33 \pm 0.46$

respect to the dimuon mass. Events in the signal mass region are grouped into independent q^2 bins. Figure 2 (a, b) shows the differential BR for $B^+ \rightarrow K^+ \mu^+ \mu^-$ and $B^0 \rightarrow K^{*0} \mu^+ \mu^-$.

The A_{FB} and the K^{*0} longitudinal polarization fraction (F_L) are extracted by an unbinned likelihood fit to the $\cos \theta_\mu$ and $\cos \theta_K$ distributions, respectively, where θ_μ is the angle between the μ^+ (μ^-) direction and the direction opposite to the B (\bar{B}) meson in the dimuon restframe, and θ_K is the angle between the kaon direction and the direction opposite to the B meson in the K^{*0} rest frame. The differential decay rates [2] are sensitive to $\cos \theta_K$ and $\cos \theta_\mu$ through the angular distributions given by $\frac{3}{2}F_L \cos^2 \theta_K + \frac{3}{4}(1 - F_L)(1 - \cos^2 \theta_K)$ for $\cos \theta_K$ and $\frac{3}{4}F_L(1 - \cos^2 \theta_\mu) + \frac{3}{8}(1 - F_L)(1 + \cos^2 \theta_\mu) + A_{FB} \cos \theta_\mu$ for $\cos \theta_\mu$. We measure F_L and A_{FB} for $B^0 \rightarrow K^{*0} \mu^+ \mu^-$ and also A_{FB} for $B^+ \rightarrow K^+ \mu^+ \mu^-$. Angular acceptances are obtained from simulated signal samples assuming unpolarized decays.

The contribution from decays with $K\pi$ swapped K^{*0} mesons distorts the signal distribution and swaps the sign of $\cos \theta_\mu$. This effect is considered by adding an additional signal-like term to the likelihood function. The contribution from decays with non-resonant $K\pi$ is considered to be small [2] and neglected in the fit. For the B^+ decay, we set $F_L = 1$ and consider no scalar term [3].

The combinatorial background PDF shape is taken from the B mass upper sideband that is used for the NN training. In the fit to $\cos \theta_K$ ($\cos \theta_\mu$) distribution, the only free parameter is F_L (A_{FB}). For the $\cos \theta_\mu$ fit, the value of F_L is fixed to the $\cos \theta_K$ fit result.

Most dominant source of systematic uncertainty for each angular fit is the fit bias near the physical boundary (0.02–0.07) for F_L in B^0 , the uncertainty of the F_L fit (0.02–0.12) for A_{FB} in B^0 , and the angular background shape (0.01–0.07) for A_{FB} in B^+ . The total systematic uncertainties lie in the range 0.02–0.08 for F_L in B^0 , 0.05–0.25 for A_{FB} in B^0 , and 0.02–0.08 for A_{FB} in B^+ . The angular fit results are shown in Fig. 2 (c, d) and summarized in Table III. Results in the range $0 \leq q^2 < 4.3 \text{ GeV}^2/c^2$ and $1 \leq q^2 < 6 \text{ GeV}^2/c^2$ are also included.

In summary, we have updated our previous analysis of the flavor-changing neutral current decays $b \rightarrow s\mu\mu$ using data corresponding to an integrated luminosity of 4.4 fb^{-1} . We report the first observation of the $B_s^0 \rightarrow \phi \mu^+ \mu^-$, the most rare B_s^0 decay observed to

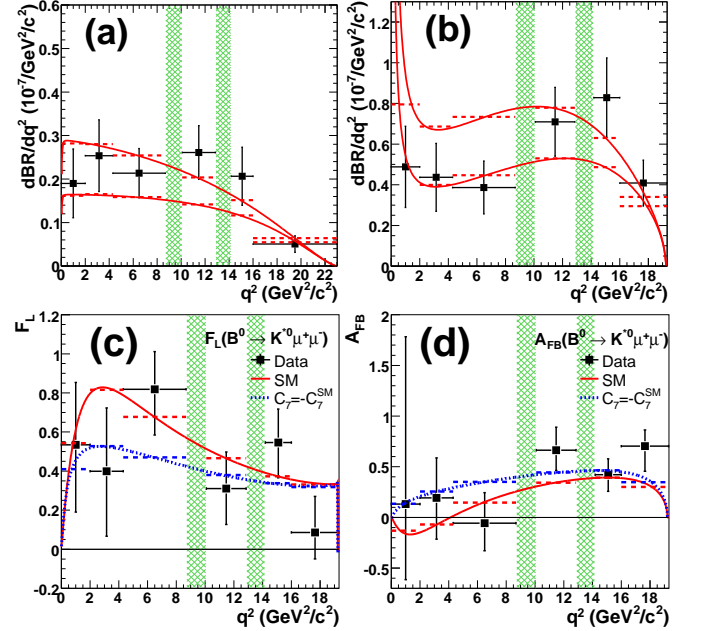


FIG. 2: Differential BR of $B^+ \rightarrow K^+ \mu^+ \mu^-$ (a) and differential BR (b), longitudinal K^{*0} polarization fraction (c), and forward-backward asymmetry (d) of $B^0 \rightarrow K^{*0} \mu^+ \mu^-$, as a function of squared dimuon mass. Points are the fit result. The solid curves are the SM expectation [1]. Two solid curves in (a, b) use maximum- and minimum- allowed form factors on differential BR plots. The dotted curves are the $C_7 = -C_7^{\text{SM}}$ expectation. The dashed line is the averaged expectation in each squared dimuon mass bin and hatched regions are charmonium veto regions.

date, and measure the total BR. We measure the total BR, differential BR, A_{FB} of the $B^+ \rightarrow K^+ \mu^+ \mu^-$ and $B^0 \rightarrow K^{*0} \mu^+ \mu^-$, with respect to q^2 . We also measure F_L of $B^0 \rightarrow K^{*0} \mu^+ \mu^-$ prior to A_{FB} . These are consistent and competitive with the other current best results. At present there is no evidence of discrepancy from the SM prediction.

We thank the Fermilab staff and the technical staffs of the participating institutions for their vital contributions. This work was supported by the U.S. Department of Energy and National Science Foundation; the Italian Istituto Nazionale di Fisica Nucleare; the Ministry of Education, Culture, Sports, Science and Technology of Japan; the Natural Sciences and Engineering Research Council of Canada; the National Science Council of the Republic of China; the Swiss National Science Foundation; the A.P. Sloan Foundation; the Bundesministerium für Bildung und Forschung, Germany; the World Class University Program, the National Research Foundation of Korea; the Science and Technology Facilities Council and the Royal Society, UK; the Institut National de Physique Nucléaire et Physique des Particules/CNRS; the Russian Foundation for Basic Research; the Minis-

TABLE III: Summary of $B^0 \rightarrow K^{*0} \mu^+ \mu^-$ and $B^+ \rightarrow K^+ \mu^+ \mu^-$ fit results. Maximum q^2 is 19.30 (23.00) GeV^2/c^2 for B^0 (B^+).

q^2 (GeV^2/c^2)	$\text{BR}(B^0)$ (10^{-7})	$F_L(B^0)$	$A_{\text{FB}}(B^0)$	$\text{BR}(B^+)$ (10^{-7})	$A_{\text{FB}}(B^+)$
[0.00, 2.00)	$0.98 \pm 0.40 \pm 0.09$	$0.53^{+0.32}_{-0.34} \pm 0.07$	$0.13^{+1.65}_{-0.75} \pm 0.25$	$0.38 \pm 0.16 \pm 0.03$	$-0.15^{+0.46}_{-0.39} \pm 0.08$
[2.00, 4.30)	$1.00 \pm 0.38 \pm 0.09$	$0.40^{+0.32}_{-0.33} \pm 0.08$	$0.19^{+0.40}_{-0.41} \pm 0.14$	$0.58 \pm 0.19 \pm 0.04$	$0.72^{+0.40}_{-0.35} \pm 0.07$
[4.30, 8.68)	$1.69 \pm 0.57 \pm 0.15$	$0.82^{+0.19}_{-0.23} \pm 0.07$	$-0.06^{+0.30}_{-0.28} \pm 0.05$	$0.93 \pm 0.25 \pm 0.06$	$-0.20^{+0.17}_{-0.28} \pm 0.03$
[10.09, 12.86)	$1.97 \pm 0.47 \pm 0.17$	$0.31^{+0.19}_{-0.18} \pm 0.02$	$0.66^{+0.23}_{-0.20} \pm 0.07$	$0.72 \pm 0.17 \pm 0.05$	$-0.10^{+0.17}_{-0.15} \pm 0.07$
[14.18, 16.00)	$1.51 \pm 0.36 \pm 0.13$	$0.55^{+0.17}_{-0.18} \pm 0.02$	$0.42^{+0.16}_{-0.16} \pm 0.09$	$0.38 \pm 0.12 \pm 0.03$	$0.03^{+0.49}_{-0.16} \pm 0.04$
[16.00, 19.30(23.00))	$1.35 \pm 0.37 \pm 0.12$	$0.09^{+0.18}_{-0.14} \pm 0.03$	$0.70^{+0.16}_{-0.25} \pm 0.10$	$0.35 \pm 0.13 \pm 0.02$	$0.07^{+0.30}_{-0.23} \pm 0.02$
[0.00, 4.30)	$1.98 \pm 0.55 \pm 0.18$	$0.47^{+0.23}_{-0.24} \pm 0.03$	$0.21^{+0.31}_{-0.33} \pm 0.05$	$0.96 \pm 0.25 \pm 0.06$	$0.36^{+0.24}_{-0.26} \pm 0.06$
[1.00, 6.00)	$1.60 \pm 0.54 \pm 0.14$	$0.50^{+0.27}_{-0.30} \pm 0.03$	$0.43^{+0.36}_{-0.37} \pm 0.06$	$1.01 \pm 0.26 \pm 0.07$	$0.08^{+0.27}_{-0.22} \pm 0.07$

terio de Ciencia e Innovación, and Programa Consolider-Ingenio 2010, Spain; the Slovak R&D Agency; and the Academy of Finland.

-
- [1] A. Ali, P. Ball, L. T. Handoko, and G. Hiller, Phys. Rev. D**61**, 074024 (2000).
[2] F. Kruger and J. Matias, Phys. Rev. D**71**, 094009 (2005).
[3] C. Bobeth, G. Hiller, and G. Piranishvili, J. High Energy Phys. 12 (2007) 040.
[4] B. Aubert *et al.* (BaBar Collaboration), Phys. Rev. D**79**, 031102 (2009); J. T. Wei *et al.* (Belle Collaboration), Phys. Rev. Lett. **103**, 171801 (2009).
[5] T. Aaltonen *et al.* (CDF Collaboration), Phys. Rev. D**79**, 011104 (2009).
[6] V. M. Abazov *et al.* (D0 Collaboration), Phys. Rev. D**74**, 031107 (2006).
[7] D. Acosta *et al.* (CDF Collaboration), Phys. Rev. D**71**,

032001 (2005).

- [8] T. Aaltonen *et al.* (CDF Collaboration), Phys. Rev. Lett. **102**, 242002 (2009), and references therein.
[9] We use a cylindrical coordinate system in which θ is the polar angles with respect to the proton beamline and pseudorapidity $\eta \equiv -\ln(\tan \theta/2)$.
[10] K. Nakamura *et al.* (Particle Data Group), J. Phys. G**37**, 075021 (2010).
[11] T. Aaltonen *et al.* (CDF Collaboration), Phys. Rev. Lett. **100**, 101802 (2008).
[12] T. Sjöstrand *et al.*, Comput. Phys. Commun. **135**, 238 (2001); D. J. Lange, Nucl. Instrum. Meth. A**462**, 152 (2001).
[13] C. Q. Geng and C. C. Liu, J. Phys. G**29**, 1103 (2003).
[14] G. Punzi, in Proc. of the Conference on Statistical Problems in Particle Physics, Astrophysics and Cosmology (Phystat 2003), (SLAC, Menlo Park, CA, 2003), p. 79.
[15] B. Aubert *et al.* (BaBar Collaboration), Phys. Rev. Lett. **102**, 091803 (2009).